Consilience and the Peripheral Sensory Adaptation Response

Willy Wong

May 1, 2021

Abstract

Measurements of the peripheral sensory adaptation response were compared to a simple mathematical relationship involving the spontaneous, peak and steady-state activities. This relationship is based on the geometric mean and is found to be obeyed to good approximation in peripheral sensory units showing a sustained response to prolonged stimulation. From an extensive review of past studies, the result was shown to be independent of modality and is satisfied in a wide range of animal species. The consilience of evidence, from nearly one hundred years of experiments beginning with the work of Edgar Adrian, suggests that this is a fundamental result of neurophysiology.

1 Introduction

Consilience is the convergence of evidence from different lines of studies or approaches [1]. The unity of science implies that results obtained by one approach should concur with evidence obtained by an entirely different approach. This principle has found utility in biology where systematic bodies of evidence can be hard to obtain. Consilience has been invoked most prominently in establishing the modern theory of evolution.

Can consilience find application in sensory physiology? While there is little debate that sensory adaptation appears universally amongst the different senses and organisms, there has been no attempt to carry out a *quantitative comparison* of adaptation responses. Some of the first experiments conducted on sensory nerve endings were carried out by Nobel Laureate Edgar Adrian. Collaborating with his assistant Yngve Zotterman, Adrian conducted one of his most celebrated experiments: the measurement of the rate of impulses from the frog muscle spindle to the stretch of a muscle [2]. What Adrian found was that the neural activity rises immediately upon initiation of the stretch and falls monotonically with time. This is now known as sensory adaptation and is observed nearly universally in all of the senses across many different organisms. A schematic representation of their finding can be found in figure 1 which includes spontaneous activity prior to the application of the stimulus (SR), the peak activity that occurs at or soon after the presentation of the stimulus (PR), and the steady-state activity after adaptation has stopped (SS).

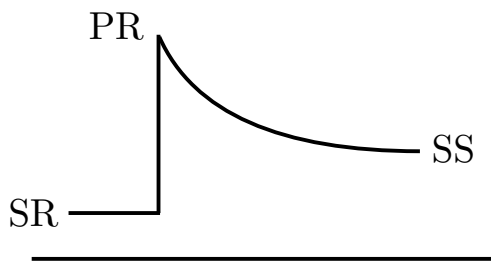

Figure 1: Peripheral sensory adaptation curve. An idealized sensory adaptation response showing steady-state spontaneous response (SR) prior to introduction of stimulus, the peak response to the stimulus (PR), and the subsequent new steady-state response (SS).

A particular pattern emerges from Adrian's studies when the results are analyzed numerically. By taking the three fixed points in the graph, we observe from his data that the steady-state activity equals the geometric mean of the peak activity and spontaneous activity. This finding is not restricted to a single one of his experiments. In the third instalment of his celebrated 1926 papers [3], Adrian and Zotterman measured adaptation in Merkel units in the footpad of a cat to pressure stimuli where a similar result can be found. In equation form, this implies that

$$\mathrm{SS} = \sqrt{\mathrm{PR} \times \mathrm{SR}} \tag{1}$$

Subsequent to Adrian's discoveries, many investigators have studied the peripheral response in other modalities and organisms. While many of the measured adaptation responses follow the same qualitative shape of figure 1, the question that remains unanswered is whether they share *quantitative similarities*. Neurons process and encode many types of information; a diversity of responses can be found at the peripheral level, some of which may even differ from the representation shown in figure 1. Notable exceptions include the rapidly adapting mechanoreceptors in touch as well as certain units involved in temperature coding. This study focuses on responses that show sustained activity with constant input in isolated peripheral sensory units. This matter is discussed later in the paper.

An exhaustive search was carried out on past studies of peripheral sensory adaptation. From these studies, results were analyzed and compared to equation (1). Despite vastly different mechanisms and modalities, and in organisms from different phyla in Animalia, equation (1) was found to be obeyed to good

approximation. From the perspective of consilience, this demonstrates that equation (1) is widely applicable and may constitute a new law of neurophysiology. The search for this equation was motivated by some recent theoretical considerations [4].

2 Results and Discussion

A brief overview of the studies analyzed. A comprehensive search was carried out in peripheral sensory adaptation yielding thirty five studies which satisfied the conditions set forth in the search criteria (see Methods). Over thirty percent of the studies were conducted within the past twenty years. At least fifteen of the studies included multiple measurements under different conditions. In total, there are 246 separate adaptation responses analyzed. The dataset spans seven of the most important sensory modalities including proprioception, touch, taste, hearing, vision, smell and temperature. A total of thirteen studies were identified to test the same modality/same animal species but were conducted in different labs. One study examined units of both high and low spontaneous activity in the same modality. There are other aspects of the data set worth noting and are discussed later.

We begin the analysis with point-wise comparisons to equation (1). Table 1 shows the results from eighteen studies which permit a single comparison of spontaneous, peak and steady-state activities. Equation (1) appears to hold well across different animal species and modalities, although the limited availability of data in each study makes it difficult to draw robust conclusions. Taken together, however, the convergence of evidence is strong. Error between predicted and measured steady-state response is generally within ten percent or less. There are some exceptions. The largest source of discrepancy was found in a study on temperature [5] where in two instances the predictions miss the measured values by a considerable amount. Temperature is particularly difficult to reconcile and is discussed in more detail later. A number of results (marked by *) are derived from so-called 'inverted' responses. These are also discussed later.

The first two datasets in table 1 are from Adrian's own pioneering work and were reconstructed using either extrapolated data (because the stimulus was not held long-enough for the response to reach steady state) [2] or by pooling data from other recordings of the same unit [3]. It would be easy to exclude these studies, but their historical significance cannot be ignored. Of additional interest is a study on hearing which compares the adaptation response of the same unit when cooled or warmed relative to body temperature (see results conducted on gerbil hearing [6]). Changes in local temperature result in spike activities differing by at least a factor of two. One could easily imagine that the three values rise or fall uniformly with a change in temperature. Instead, they move in a direction to preserve the equality of the geometric mean. This has possible implications for the generality of the relationship across different animal species where metabolic activity can differ widely. One study was conducted on the visual sensory structures of the jellyfish (rhopalia) by measuring the output of pacemaker cells [7]. The rhopalia modulates directly the output of these cells which determines the basic swim movement in jellyfish [7, 8].

Table 1: A summary of different peripheral sensory adaptation results highlighting the relationship between spontaneous, peak and steady-state activities for different modalities and organisms. *Indicates data derived from an inverted adaptation response.

Spontaneous (SR, Hz)	Peak (PR, Hz)	Steady-state (SS, Hz)	Prediction (Hz)	Modality	Organism	Source
6.1	26.8	13.2	12.8	Proprioception	Frog	Figure 10B (exp. 12) [2]
3.7	99.7	19.3	19.2	Touch	Cat	Figure 8 (exp. 6) [3]
15.4	59.9	25.9	30.4	Proprioception	Cat	Figure 3 (filled circles, prep. 52) [9]
14.1*	9.1*	11.0*	11.3*	Proprioception	Cat	Figure 3 (open circles, stimulus on, prep. 52) [9]
11.0*	16.9*	13.8*	13.6*	Proprioception	Cat	Figure 3 (open circles, stimulus off, prep. 52) [9]
12.9	31.1	18.9	20.0	Proprioception	Cat	Figure 4 (initial adaptation, prep. 54) [9]
37.7	151	81.7	75.4	Hearing	Cat	Figure 6.6 (unit 297-43) [10]
60.1	179	100	104	Hearing	Cat	Figure 6.7 (unit 299-22) [10]
28.8	70.7	44.6	45.1	Proprioception	Cat	Figure 7 (first adaptation) [11]
44.6*	18.1*	33.4*	28.4*	Proprioception	Cat	Figure 7 (second adaptation) [11]
33.4	65.1	43.7	46.6	Proprioception	Cat	Figure 7 (third adaptation) [11]
43.7*	16.4*	28.0*	26.8*	Proprioception	Cat	Figure 7 (fourth adaptation) [11]
28.0	57.8	42.4	40.2	Proprioception	Cat	Figure 7 (fifth adaptation) [11]
42.4*	13.4 *	22.9*	23.8*	Proprioception	Cat	Figure 7 (sixth adaptation) [11]
23.9	43.4	32.0	32.2	Proprioception	Cat	Figure 8 (first adaptation) [11]
32.0*	8.9*	23.3*	16.9 *	Proprioception	Cat	Figure 8 (second adaptation) [11]
23.3	43.4	30.7	31.8	Proprioception	Cat	Figure 8 (third adaptation) [11]
30.7*	11.2*	22.9*	18.5*	Proprioception	Cat	Figure 8 (fourth adaptation) [11]
22.9	42.0	31.6	31.0	Proprioception	Cat	Figure 8 (fifth adaptation) [11]
31.6*	7.9*	23.0*	15.8*	Proprioception	Cat	Figure 8 (sixth adaptation) [11]
23.0	42.0	30.9	31.1	Proprioception	Cat	Figure 8 (seventh adaptation) [11]
6.7	22.6	10.9	12.3	Touch	Cat	Figure 2B (adaptation) [12]
10.9*	1.9*	6.7*	4.6*	Touch	Cat	Figure 2B (recovery) [12]
2.7	16.3	7.4	6.6	Vision	Squid	Figure 1b [13]
8.5	67.9	23.6	24.0	Smell	Mosquito	Figure 2 (top) [14]
11.7	69.6	30.6	28.5	Smell	Mosquito	Figure 2 (bottom, middle presentation) [14]
13.6	81.0	29.5	33.2	Taste	Rat	Figure 2 (initial adaptation) [15]
4.9	27.5	11.6	12.4	Proprioception	Crayfish	Figure 1 [16]
12.2	96.1	28.7	34.2	Hearing (warm)	Gerbil	Figure 1 (upper) [6]
2.6	51.1	14.5	11.5	Hearing (cool)	Gerbil	Figure 1 (lower) [6]
6.1	199	30.5	34.8	Smell	Fruit fly	Figure 11A (first presentation) [17]
3.8	199	28.8	27.5	Smell	Fruit fly	Figure 11C (middle presentation) [17]

1.8	9.9	4.0	4.2	Proprioception	Cockroach	Figure A i [18]
3.8	199	28.8	27.5	Proprioception	Cockroach	Figure A ii [18]
17.0	144	33.4	49.4	Temperature	Beetle	Figure 10A [5]
4.6	278	21.2	35.8	Temperature	Beetle	Figure 10B [5]
2.3	333	26.1	27.6	Temperature	Beetle	Figure 10C [5]
2.4	15.0	7.7	6.0	Smell	Fish	Figure 1a (Lys) [19]
4.9	70.0	22.3	18.5	Smell	Fish	Figure 1c (Trp) [19]
3.1	73.2	24.2	15 .1	Smell	Fish	Figure 1c (Trp, 50 min. later) [19]
7.8	61.4	19.1	21.9	Temperature	Mosquito	Figure 2A [20]
3.3*	15.0*	7.6*	7.0*	Temperature	Mosquito	Figure 2B [20]
0.14*	2.0*	0.58*	0.53*	Vision	Jellyfish	Figure 3D [7]
1.1	2.1	1.5	1.5	Vision	Jellyfish	Figure 4D [7]
1.5	40.0	7.4	7.7	Vibration	Fish	Figure 2 [21]
5.6	104	28.9	24.1	Vibration	Fish	Figure 5a [21]
26.5	71.6	42.2	43.6	Vibration	Fish	Figure 5b [21]

The unfortunate circumstance is that spontaneous activity is not always reported or shown. However, this can be overcome if the adaptation response is measured to multiple stimulus levels. Since spontaneous activity is the activity in the *absence of stimulation*, its value is independent of intensity. As such, equation (1) predicts a square root relationship between peak and steady-state activity which, on a double-log plot, is a straight line with slope 1/2 and value of intercept dependent on the level of spontaneous activity. See Appendix A for mathematical details. Figure 2 shows the results from fourteen studies conducted at different levels of intensity. Multiple measurements from the same unit increase the robustness of the findings. In total, this figure comprises over 170 separate adaptation responses. Panels (a)-(h) show responses from mechanoreception, (i)-(m) chemoreception, (n) thermoreception, and (o) photoreception. Regression analysis is detailed in Appendix A. From the entirety of the data in figure 2, a single common value of slope was found to be 0.662.

Of particular interest are panels (a) and (c) which show measurements taken from the same animal/modality (guinea pig hearing) conducted in different labs separated by almost ten years apart. Panel (c) shows the response of four fibres, including two with low spontaneous activity and two with high spontaneous activity. In all cases, the power law relationship is preserved, with those units with high spontaneous activity having a higher value of intercept than those with low spontaneous activity. Panels (a)-(d) show mammalian hearing mediated via the cochlear while panel (e) shows hearing in the fish mediated via the otolith. In (f), we observe the response of the fish lateral line. Panels (h) and (i) show the taste response in a blowfly to five alkali salts at different intensities. In total, there are forty eight measurements from two units. Although the data are shown with offset, the actual values overlap indicating that they share a similar slope and intercept – which is not surprising given the common value of spontaneous activity. The last panel (o) differs from the other studies in that adaptation was conducted *on top* of an existing pedestal. That is, the retinal ganglion cell was adapted to an existing level of luminance before responding to a further increment. Despite the change in test condition, the quantitative aspects of the response remain unchanged.

Adaptation responses measured from ascending and descending staircases allow for further testing of equation (1) to *pre-adapted levels*. A stimulus staircase is a series of ascending and/or descending intensity steps. Several studies have made use of stimulus staircases including: measurements from warm units in the cat [34] and bat [35] to increasingly warmer temperatures; recordings from M1 cells for non-image-based vision (i.e. intrinsically photosensitive retinal ganglion cells or ipRGC's) in mice to light of increasing levels [36]; measurements from olfactory sensory neurons of fruit flies to ascending and descending levels of acetone concentrations [37]. The data from four studies together with the predicted values are shown in figure 3. Taken together, this suggests the following generalization of equation (1):

$$\mathrm{SS}_{\mathrm{final}} = \sqrt{\mathrm{PR} \times \mathrm{SS}_{\mathrm{initial}}} \tag{2}$$

This equation includes equation (1) as a special case.

While adaptation responses commonly conform to the schematic representation shown in figure 1, there are also circumstances where the response is inverted from its usual representation. The most common form of an 'inverted' response is the recovery after the removal of the stimulus. The response falls before returning to the original value prior to the application of the stimulus. Certain units also exhibit a fully inverted response. These are referred to as inhibitory responses, and can be observed in, say, [20] where a warm and cool temperature receptor are presented with the same stimulus: The warm unit follows the typical adaptation response to a rise in temperature while the cool unit falls with the same temperature increase. Inhibitory responses are also commonly found in other modalities. Regardless of the shape of the response, the salient point is that equation (2) is obeyed not just for conventional adaptation but for the inverted response as well. A number of inverted responses are included in the dataset: see recovery and inhibitory responses in figure 1 (values marked with *) and the response to a descending stimulus staircase for odour [37] and temperature [38] in figure 3.

All of this suggests that there is a higher organizational principle underlying peripheral sensory adaptation. What sort of theory or model of transduction would be compatible with equation (2)? There are a number of models, particularly in hearing, that provide good compatibility to experimental data recorded from single unit activity [39, 40]. However, since the geometric mean relationship appears to hold across

different modalities, it is not reasonable to expect a modality-specific model to be extended to work with other modalities without additional, possibly ad hoc, assumptions. Instead the existence of equation (1) was predicted by a theory of sensory processing under development for the past fifty years. The derivation of equation (1) is provided in Appendix B and has been detailed fully elsewhere [4].

Few studies were found to be in complete violation of equation (1). Those that were are most commonly found in thermoreception. Not only are the responses predicted poorly in table 1 (see results for the beetle), but the slope of the data in panel (n) of figure 2 falls short of the predicted value of 0.5. There are also cases where the three fixed points (spontaneous, peak and steady-state) cannot be easily identified from the adaptation response [5]. Some studies also show non-monotonic behaviour with changing stimulus levels [35, 38, 41]. While certain responses do fit well (warming tends to be better), on the balance, thermoreception appears to violate equation (1). There are results from other modalities which were also found to be problematic. One study concerns the taste of blowflies [42]; however, the data in this case was obtained by averaging the response of different sensilla resulting in a non-monotonic adaptation curve. Another study, again concerning taste, shows data for sucrose and salt satisfying equation (1), but not for pheromones [43]. Apart from temperature, however, studies in violation of equation (1) are few in numbers.

Much of this study has focused on units that adapt slowly and show a sustained response to continued stimulation. Phasic receptors are rapidly adapting units that do not conform to the representation in figure 1. It is believed that phasic units respond to the rate of change of stimulus [44]. A test can be carried out to see if phasic units obey the geometric mean relationship by presenting a time-varying stimulus to induce a sustained response. This was attempted in [45] where the vestibular units of monkeys were subjected to centrifugal forces and an adaptation response was induced to a constant force stimulus. While two of the adaptation responses compare favourably to the equation (unit 213-28: $\mathrm{SS}_{meas} = 80.3$, $\mathrm{SS}_{pred} = 86.8$; unit 206-18: $\mathrm{SS}_{meas} = 125$, $\mathrm{SS}_{pred} = 130$), the paper also cites data from units which show far less levels of adaptation (unit 213-28: $\mathrm{SS}_{meas} = 97.0$, $\mathrm{SS}_{pred} = 67.6$). Moreover, the geometric mean relationship is only satisfied in the activity of *isolated* sensory units in the absence of interaction from other cells in the neural circuitry. Any neurons that are part of (say) the descending auditory pathway clearly do not follow the geometric mean relationship (e.g. see the auditory interneuron response [46] or the response of cochlear nucleus units [47]). Even within retinal ganglion cells, if the visual signal overlaps both the centre and surrounding regions (thereby recruiting inhibition), this will facilitate responses which deviate from equation (1), e.g. [48].

The main result of this paper is a relationship connecting three fixed points in the adaptation curve. No consideration was made of the time-course of adaptation. And yet, an important point of discussion in the literature is the rate at which adaptation occurs. Adaptation curves are often fitted to a sum of exponentials with different time constants, e.g. [23, 6]. More recently, it has been proposed that neuronal adaptation can be better modelled using a power-law function of time [49]. This then brings to mind whether equation (1) is compatible with such a formulation. It is important to remember that in both an exponential and a power-law description, a constant offset is required. This offset accounts for the non-zero activity when the stimulus is applied over long periods of time, e.g. see implementation of power law dynamics in [40]. As such, equation (1) is not affected by the time-course of adaptation.

While the analysis in this paper has involved the review of hundreds of publications, it is virtually impossible to capture all studies that have included measurements of an adaptation response. And yet, even with the studies considered, the convergence of evidence is striking. More than 200 measurements taken from different branches of sensory physiology are shown to be compatible with a single equation. These studies span different experimental preparations, different methods of stimulation, and may even require different techniques to measure the response. That the results would conform, even approximately, to the same mathematical relationship is remarkable and illustrates the true nature of consilience. A number of investigators have also engaged in testing the same modality-same species combination. Since these studies are conducted independently, and are shown to obey a similar mathematical relationship, this speaks to the reliability of the methodologies used. Table 2 shows a summary of studies organized by animal species. The survey of studies also serves to illustrate the historical development of the sensory sciences which followed the technological developments unfolding in the twentieth century. For example, the proprioceptive and touch

Table 2: Summary of studies analyzed organized by animal classification.

Phylum	Organism	Modality and Source
Chordata	Bat	Temperature [35]
	Cat	Touch [3, 12], proprioception [9, 11], hearing [10], vision [33], temperature [34]
	Ferret	Hearing [25]
	Fish	Hearing [26], smell [19], vibration [21]
	Frog	Proprioception [2, 28]
	Gerbil	Hearing [23, 6]
	Guinea pig	Hearing [22, 24]
	Mouse	Non-image based vision [36]
	Pigeon	Temperature [38]
	Rat	Taste [15]
Arthropoda	Beetle	Temperature [5]
	Blowfly	Taste [32]
	Caterpillar	Taste [31]
	Cockroach	Proprioception [18]
	Crayfish	Proprioception [27, 16]
	Fruit fly	Smell [17, 37, 29], taste [30]
	Mosquito	Smell [14], temperature [20]
Mollusca	Squid	Vision [13]
Cnidaria	Jellyfish	Vision [7]

senses were among the first to be investigated as they were the easiest to access and their spike activity slow enough so that reliable spike counts could be achieved even back in Adrian's time using vacuum tube amplifiers [50]. With the advent of computers and greater access to more invasive regions, the study of hearing and vision with their higher firing rates became possible. Finally, taste, olfaction and temperature came relatively later due to the difficulty in controlling and maintaining the level of stimulation. This may be one reason why the mechanoreception response shows a higher degree of conformity to equation (1) than chemoreception where the variability can be high. Nevertheless, it is fascinating to observe that the data recorded in 1926 by Adrian and Zottermann hold almost the same fidelity as modern recordings.

Quoting Paul Willis: "Consilience means to use several different lines of inquiry that converge on the same or similar conclusions. The more independent investigations you have that reach the same result, the more confidence you can have that the conclusion is correct. Moreover, if one independent investigation produces a result that is at odds with the consilience of several other investigations, that is an indication that the error is probably in the methods of the adherent investigation, not in the conclusions of the consilience." [51] This work comprises a study of enormous breadth showing, perhaps for the first time, commonalities that exists across almost all sensory modalities and animal species. Evidence includes nearly 100 years of data from seven major sensory modalities, derived from organisms from four major phyla in Animalia (see table 2). Regardless of mechanism or modality, or from which time period the study was conducted, the consilience of evidence lends proof to a new fundamental result of neurophysiology.

3 Methods

A search of peripheral sensory adaptation studies was conducted in academic databases (Google Scholar, Web of Science and PubMed) casting a wide net using various combination of keywords including *sense, sensory, adapt, adaptation, fibre, unit, receptor, neuron, afferent, tonic, peripheral, action potential, impulse, spike, inter-spike, interval, ISI, frequency, firing, rate, discharge, activity, PST, PSTH, PETH, peri-event, post-stimulus, histogram, spontaneous, coding, pedestal, staircase, recovery, coding.* Organism-specific terms like

sensillum or *sensilla* were also used, as were modality specific terms like *mechanoreception, chemoreception, thermoreception and photoreception.* Studies were also found through the tracking of citations. The following inclusion criteria was used:

- Measurements conducted on *peripheral sensory neurons*
- Unit stimulated with natural stimuli within its normal sensitivity range
- Stimulus onset is near instantaneous; stimulus is of sufficient length to achieve a steady-state response
- Spontaneous, peak and steady-state responses are reported; otherwise, if no spontaneous activity is provided, adaptation response is measured to multiple stimulus levels

In certain cases, restrictions were also relaxed to allow a greater number of studies to be included.

Data were digitized and extracted from original publications. The extracted data is available in the Supplementary Materials. For certain studies, additional steps were required. For [2], the stimulus was not held for a long enough period to achieve steady-state. Hence, the data from the peak until the removal of stimulus were fitted to an exponential plus offset equation: $c_1 \exp\left[-c_2\left(t-t'\right)\right]+c_3$ where t' is the location of the peak and c_1, c_2 and c_3 are unknown parameters to be determined by a non-linear fitting procedure carried out in MATLAB R2020a (MathWorks) using the function `nlinfit`. From here the value of c_3 was inferred to be the steady-state activity. For [3], the steady-state value was estimated using another experiment conducted on the same unit, but with a slower stimulus ramp (crosses from Fig. 8 of Exp. 6). Other studies have shown that the steady-state activity does not depend on the speed of the ramp, e.g. see [9]. In [28], the 6% stretch was not included as the steady-state value was not provided. For [27], the peak values were obtained from figure 1, but the steady-state values were obtained from figure 2. In [24], only the adaptation values conducted at 5 and 10 dB were extracted for unit GP27/04 as both the 15 and 20 dB experiments show peak responses exceeding the limit of the graph (as noted by the study authors themselves). In [35], the spontaneous activity was missing and only three of four staircase levels were included. For [5], many of the responses do not show clear values for spontaneous, peak and steady-state activities. As such, only the data of figure 10 was considered. For [7], almost all eyes show responses which conform to equation (1). However some responses took a long time to reach steady-state, and thus only the data from the lower lens eye (figure 3) and upper lens eye (figure 4) were included. For [29], several of the responses overlapped making it difficult to track their exact values particularly for the lower intensities. In [36], values were extracted only where there was a clear steady-state level of activity attained, and that the input level lies within the sensitivity range of the unit. This included the third to seventh levels of the luminance staircase in Fig. 1b and the fourth to sixth levels in Fig. 1c.

It is also instructive to examine why certain datasets could not be included in the analysis. Some studies use large bin widths to calculate firing rates thereby obscuring the fine structure in adaptation, e.g. [52]. Large bin widths reduce the noisiness of the response, at the expense of reducing the value of peak activity. Other studies subtract away the spontaneous activity from the adaptation data, e.g. [9]. Finally, a good number of studies show responses which have not yet reached steady-state before the recording was terminated or the stimulus turned off. This is perhaps the single most significant reason why certain datasets could not be included, e.g. [22, 19]. Or, if they were included e.g. [32, 29], this introduced bias in the analysis. See discussion in Appendix A.

4 Conclusion

Evidence was collected from nearly 100 years of studies on peripheral sensory adaptation. With few exceptions, independent of modality or animal species, the steady-state firing rate response was found to be equal to the geometric mean of spontaneous activity and peak activity just after stimulus onset. Further evidence suggests that this result can be generalized to the transient response to any step change in stimulus. The consilience of evidence points to a new organizational principle underlying the processing of information by sensory neurons.

A Regression analysis

An analysis of linear least squares was conducted on the data shown in figure 2. First, a fit was conducted on each dataset separately with the equation

$$\log_{10}(\mathrm{SS}) = \beta_0 + \beta_1 \log_{10}(\mathrm{PR}) \tag{3}$$

where β_1 is the slope and β_0 the intercept. SS is the steady-state activity and PR the peak activity. If the data conforms to equation (1) then $\beta_1 = 0.5$ and $\beta_0 = 0.5 \log_{10}(\mathrm{SR})$, i.e. the base 10 logarithm of spontaneous activity. Since PR is independent of intensity, β_0 is constant. Table 3 shows the results of the analysis carried out in MATLAB R2020a (MathWorks). In one dataset (figure 2, panel c, crosses [24]), there were only two points and thus the results are marked with 'NA'. The analysis shows a significant relationship between peak activity PR and steady-state activity SS (mostly $p < 0.01$), with much of the variation explained by the independent variable (mostly $R^2 > 0.9$). The confidence interval of the slope however overlapped the predicted value of 0.5 for only 50% of the datasets.

Next, we tested the hypothesis that all datasets share the same value of slope. A pairwise difference was evaluated together with the corresponding 95% confidence interval. Finally, the interval was checked to see if it overlapped the origin. Unfortunately, this happened in only two thirds of the cases meaning that there is considerable variation in the slope. Therefore, it would be difficult to conclude that all datasets share the same slope.

What is the reason for the discrepancy? Beyond the usual sources of error in measuring spike activity, there is one aspect of the data collection process that has not been addressed. Steady state activity is defined as the activity after which adaptation has stopped. However, as has been noted before, e.g. [24], adaptation curves take longer to reach steady-state when initiated with larger intensities. The consequence of this is significant. Since adaptation is measured from fixed duration presentations, the value of SS obtained from the final portion of the curve may not have reached steady-state, particularly for the higher intensities. The discrepancy will also increase as intensity is increased. From this, we conclude that there can be overestimation of the slope. For example, both [29] and [32] show responses that have yet to reach steady-state. This is reflected in the upward rise in points at the higher firing frequencies due to the higher values of steady-state activities for panels (i) and (m) in figure 2.

Nevertheless, if we assume that the values of the slopes are homogeneous (i.e. belonging to the same group), we can fit all of the data to a common slope. This was accomplished through a simultaneous curve-fit with equal weights using a different intercept for each dataset. A single value of 0.662 was obtained.

B Derivation of Equation (1)

A recent publication detailed the following equations governing the response of peripheral sensory neurons to time-varying stimulation [4]. The theory is based on a mechanism-free approach to sensory information processing:

$$F = kH \tag{4}$$

$$H = \frac{1}{2} \log\left(1 + \frac{\beta\,(I + \delta I)^p}{m}\right) \tag{5}$$

$$\frac{dm}{dt} = -a(m - m_{eq}) \tag{6}$$

$$m_{eq} = (I + \delta I)^{p/2} \tag{7}$$

where the firing rate response of the neuron F is related to the information or entropy of the stimulus H obtained by sampling a signal with intensity I. $m(t)$ is the sample size and m_{eq} the optimal value of the sample size. m_{eq} has dependency on stimulus intensity through equation (7). k, β, p, a and δI are fixed parameters. The theory has been shown to work well with many time-varying inputs for different sensory

Table 3: Regression analysis of figure 2.

Slope	Intercept	R^2	p	Panel (figure 2)	Source
0.657	0.558	0.944	< 0.01	(a)	Figure 1, unit GP-17-4 [22]
0.404	0.755	0.977	< 0.01	(b)	Figure 1, unit E8F2 [23]
0.754	-0.0415	0.998	< 0.01	(c) circles	Figure 1, unit GP31/08 [24]
0.469	1.02	0.943	< 0.05	(c) triangles	Figure 2, unit GP27/18 [24]
0.575	0.436	NA	NA	(c) crosses	Figure 1, GP31/13 [24]
0.523	0.843	0.990	< 0.01	(c) plusses	Figure 2, GP27/04 [24]
0.339	1.27	0.886	< 0.1	(d)	Figure 6 [25]
0.691	0.323	0.919	< 0.01	(e)	Figure 3, increment [26]
0.451	0.790	0.998	< 0.05	(f)	Figure 6 [21]
0.646	0.0431	0.994	< 0.01	(g)	Figures 1 and 2 [27]
0.291	0.590	0.856	< 0.01	(h)	Figure 3 [28]
0.740	0.227	0.962	< 0.01	(i) crosses	Figure 3a [29]
0.750	0.212	0.877	< 0.01	(i) triangles	Figure 5 [29]
0.865	0.00965	0.988	< 0.01	(i) circles	Figure 5 [29]
0.717	0.402	0.951	< 0.01	(i) squares	Figure 5 [29]
0.857	-0.0127	0.932	< 0.01	(i) plusses	Figure 5 [29]
0.291	0.997	0.744	< 0.1	(j)	Figure 3 [30]
0.288	0.858	0.294	< 0.4	(j)	Figure 7 [30]
0.805	0.0428	0.801	< 0.2	(k)	Figure 3 [31]
0.706	0.271	0.994	< 0.01	(l) crosses	Figure 2a, LiCl [32]
0.754	0.135	0.997	< 0.01	(l) triangles	Figure 2a, NaCl [32]
0.935	-0.347	0.988	< 0.01	(l) circles	Figure 2a, KCl [32]
0.537	0.620	0.975	< 0.01	(l) squares	Figure 2a, RbCl [32]
0.448	0.761	0.964	< 0.01	(l) plusses	Figure 2a, CsCl [32]
0.808	-0.352	0.975	< 0.01	(m) crosses	Figure 2b, LiCl [32]
0.754	-0.216	0.990	< 0.01	(m) triangles	Figure 2b, NaCl [32]
0.941	-0.806	0.977	< 0.01	(m) circles	Figure 2b, KCl [32]
1.06	-1.145	0.979	< 0.01	(m) squares	Figure 2b, RbCl [32]
0.579	0.118	0.927	< 0.01	(m) plusses	Figure 2b, CsCl [32]
0.293	0.630	0.826	< 0.1	(n) circles	Figure 10 [5]
0.650	0.439	0.966	< 0.01	(o) circles	Figure 7, $1 \times 10^{-5}\,\mathrm{cd\,m^{-2}}$ [33]
0.321	1.26	0.967	< 0.01	(o) triangles	Figure 7, $1 \times 10^{-3}\,\mathrm{cd\,m^{-2}}$ [33]
0.415	0.966	0.982	< 0.01	(o) crosses	Figure 7, $1 \times 10^{-1}\,\mathrm{cd\,m^{-2}}$ [33]

modalities and organisms. The equations are not difficult to solve, requiring only a solution to a first-order ordinary differential equation. Moreover, they can be solved even more simply numerically using less than ten lines of computer code. Sample code is provided in the Supplemental Materials.

The following is an abbreviated derivation of equation (1); please see [4] for more details. We begin by solving the response to a step input to obtain the adaptation curve. Given an input that is zero for $t < 0$ and I for $t > 0$, equation (6) can be solved to be

$$m(t) = \delta I^{p/2} e^{-at} + (I + \delta I)^{p/2} \left[1 - e^{-at}\right] \tag{8}$$

where the continuity of the solution requires the initial condition to be $m(0) = \delta I^{p/2}$. Substituting $m(t)$ into H and F gives the familiar monotonic decay behaviour observed in figure 1. See Supplemental Material for the equivalent numerical solution.

The simplicity of equation (1) implies that it is likely the result of some approximation. Consider the case where $\beta\,(I + \delta I)^p / m \ll 1$ in equation (5). This is satisfied when the parameters are small in value (e.g. $\beta \ll 1$) or when the unit is stimulated with lower intensity values, or a combination of both. In this case,

we can approximate (5) through a first-order Taylor series expansion. Together with (4), we obtain

$$F = \frac{(I + \delta I)^p}{m}$$

where we have set $k\beta = 2$. The values of these constants are not important for this discussion. We are now ready to derive equation (1).

For spontaneous activity, the input intensity is zero and $m = \delta I^{p/2}$. At stimulus onset, the intensity has value I and $m = \delta I^{p/2}$ through evaluation of equation (8) at $t = 0$. Finally, for steady-state, we evaluate (8) at $t \to \infty$ to obtain $m = (I + \delta I)^{p/2}$. This gives

$$\begin{aligned} \mathrm{SR} &= \delta I^{p/2} \\ \mathrm{PR} &= \frac{(I + \delta I)^p}{\delta I^{p/2}} \\ \mathrm{SS} &= (I + \delta I)^{p/2} \end{aligned}$$

from which we easily obtain equation (1). A similar method can be used to derive equation (2), as well as a corresponding equation for the inverted response.

References

[1] Wilson EO. 1999 *Consilience: The Unity of Knowledge*. Vintage.

[2] Adrian ED, Zotterman Y. 1926a The impulses produced by sensory nerve-endings: Part 2. The response of a Single End-Organ. *Journal of Physiology* **61**, 151–171.

[3] Adrian ED, Zotterman Y. 1926b The impulses produced by sensory nerve endings: Part 3. Impulses set up by Touch and Pressure. *Journal of Physiology* **61**, 465–483.

[4] Wong W. 2020 On the rate coding response of peripheral sensory neurons. *Biological Cybernetics* **114**, 609–619.

[5] Merivee E, Vanatoa A, Luik A, Rahi M, Sammelselg V, Ploomi A. 2003 Electrophysiological identification of cold receptors on the antennae of the ground beetle *Pterostichus aethiops*. *Physiological Entomology* **28**, 88–96.

[6] Ohlemiller KK, Siegel JH. 1998 Temporal aspects of the effects of cooling on responses of single auditory nerve fibers. *Hearing Research* **123**, 78–86.

[7] Garm A, Mori S. 2009 Multiple photoreceptor systems control the swim pacemaker activity in box jellyfish. *Journal of Experimental Biology* **212**, 3951–3960.

[8] Katsuki T, Greenspan RJ. 2013 Jellyfish nervous systems. *Current Biology* **23**, R592–R594.

[9] Boyd I, Roberts T. 1953 Proprioceptive discharges from stretch-receptors in the knee-joint of the cat. *Journal of Physiology* **122**, 38–58.

[10] Kiang NYS. 1965 *Discharge Patterns of Single Fibers in the Cat's Auditory Nerve*. MIT Press, Cambridge.

[11] Matthews P, Stein R. 1969 The sensitivity of muscle spindle afferents to small sinusoidal changes of length. *Journal of Physiology* **200**, 723–743.

[12] Chambers MR, Andres K, Duering Mv, Iggo A. 1972 The structure and function of the slowly adapting type II mechanoreceptor in hairy skin. *Quarterly Journal of Experimental Physiology and Cognate Medical Sciences: Translation and Integration* **57**, 417–445.

[13] Lange GD, Hartline PH. 1974 Retinal responses in squid and octopus. *Journal of Comparative Physiology* **93**, 19–36.

[14] Davis EE. 1976 A receptor sensitive to oviposition site attractants on the antennae of the mosquito, *Aedes aegypti*. *Journal of Insect Physiology* **22**, 1371–1376.

[15] Smith DV, Bealer SL, Van Buskirk RL. 1978 Adaptation and recovery of the rat chorda tympani response to NaCl. *Physiology & Behavior* **20**, 629–636.

[16] Barrio L, Buño W, Segundo J. 1988 Sensory-synaptic interactions in crayfish stretch receptor neurones. *Biological Cybernetics* **59**, 385–394.

[17] De Bruyne M, Clyne PJ, Carlson JR. 1999 Odor coding in a model olfactory organ: The *Drosophila* maxillary palp. *Journal of Neuroscience* **19**, 4520–4532.

[18] Ridgel A, Frazier S, DiCaprio R, Zill S. 2000 Encoding of forces by cockroach tibial campaniform sensilla: implications in dynamic control of posture and locomotion. *Journal of Comparative Physiology A* **186**, 359–374.

[19] Friedrich RW, Laurent G. 2004 Dynamics of olfactory bulb input and output activity during odor stimulation in zebrafish. *Journal of Neurophysiology* **91**, 2658–2669.

[20] Gingl E, Hinterwirth A, Tichy H. 2005 Sensory representation of temperature in mosquito warm and cold cells. *Journal of Neurophysiology* **94**, 176–185.

[21] Mogdans J, Müller C, Frings M, Raap F. 2017 Adaptive responses of peripheral lateral line nerve fibres to sinusoidal wave stimuli. *Journal of Comparative Physiology A* **203**, 329–342.

[22] Smith RL, Zwislocki J. 1975 Short-term adaptation and incremental responses of single auditory-nerve fibers. *Biological Cybernetics* **17**, 169–182.

[23] Westerman LA, Smith RL. 1984 Rapid and short-term adaptation in auditory nerve responses. *Hearing Research* **15**, 249–260.

[24] Yates GK, Robertson D, Johnstone BM. 1985 Very rapid adaptation in the guinea pig auditory nerve. *Hearing Research* **17**, 1–12.

[25] Sumner CJ, Palmer AR. 2012 Auditory nerve fibre responses in the ferret. *European Journal of Neuroscience* **36**, 2428–2439.

[26] Fay RR. 1985 Sound intensity processing by the goldfish. *Journal of the Acoustical Society of America* **78**, 1296–1309.

[27] Brown M, Stein R. 1966 Quantitative studies on the slowly adapting stretch receptor of the crayfish. *Kybernetik* **3**, 175–185.

[28] Loewenstein WR. 1956 Excitation and changes in adaptation by stretch of mechanoreceptors. *Journal of Physiology* **133**, 588–602.

[29] Martelli C, Carlson JR, Emonet T. 2013 Intensity invariant dynamics and odor-specific latencies in olfactory receptor neuron response. *Journal of Neuroscience* **33**, 6285–6297.

[30] Gothilf S, Galun R, Bar-Zeev M. 1971 Taste reception in the Mediterranean fruit fly: Electrophysiological and behavioural studies. *Journal of Insect Physiology* **17**, 1371–1384.

[31] Bernays E, Chapman R, Hartmann T. 2002 A highly sensitive taste receptor cell for pyrrolizidine alkaloids in the lateral galeal sensillum of a polyphagous caterpillar, *Estigmene acraea*. *Journal of Comparative Physiology A* **188**, 715–723.

[32] Maes F, Harms G. 1986 Neural coding of salt taste quality in the blowfly *Calliphora vicina*. *Journal of Comparative Physiology A* **159**, 75–88.

[33] Sakmann B, Creutzfeldt OD. 1969 Scotopic and mesopic light adaptation in the cat's retina. *Pflügers Archiv* **313**, 168–185.

[34] Handwerker HO, Neher KD. 1976 Characteristics of C-fibre receptors in the cat's foot responding to stepwise increase of skin temperature to noxious levels. *Pflügers Archiv* **365**, 221–229.

[35] Schäfer K, Braun HA, Kürten L. 1988 Analysis of cold and warm receptor activity in vampire bats and mice. *Pflügers Archiv* **412**, 188–194.

[36] Milner ES, Do MTH. 2017 A population representation of absolute light intensity in the mammalian retina. *Cell* **171**, 865–876.

[37] Kim AJ, Lazar AA, Slutskiy YB. 2011 System identification of Drosophila olfactory sensory neurons. *Journal of Computational Neuroscience* **30**, 143–161.

[38] Schäfer K, Necker R, Braun HA. 1989 Analysis of avian cold receptor function. *Brain Research* **501**, 66–72.

[39] Sumner CJ, Lopez-Poveda EA, O'Mard LP, Meddis R. 2003 Adaptation in a revised inner-hair cell model. *Journal of the Acoustical Society of America* **113**, 893–901.

[40] Zilany MS, Bruce IC, Nelson PC, Carney LH. 2009 A phenomenological model of the synapse between the inner hair cell and auditory nerve: Long-term adaptation with power-law dynamics. *Journal of the Acoustical Society of America* **126**, 2390–2412.

[41] Heinz M, Schäfer K, Braun HA. 1990 Analysis of facial cold receptor activity in the rat. *Brain Research* **521**, 289–295.

[42] Dethier V, Bowdan E. 1984 Relations between differential threshold and sugar receptor mechanisms in the blowfly.. *Behavioral neuroscience* **98**, 791.

[43] Bowdan E. 1984 Electrophysiological responses of tarsal contact chemoreceptors of the apple maggot fly Rhagoletis pomonella to salt, sucrose and oviposition-deterrent pheromone. *Journal of Comparative Physiology A* **154**, 143–152.

[44] Binder MD, Hirokawa N, Windhorst U, editors. 2009 pp. 54–54. In *Adaptation of Sensory Receptors*, pp. 54–54. Berlin, Heidelberg: Springer Berlin Heidelberg.

[45] Fernández C, Goldberg JM. 1976 Physiology of peripheral neurons innervating otolith organs of the squirrel monkey. I. Response to static tilts and to long-duration centrifugal force. *Journal of Neurophysiology* **39**, 970–984.

[46] Hildebrandt KJ, Benda J, Hennig RM. 2009 The origin of adaptation in the auditory pathway of locusts is specific to cell type and function. *Journal of Neuroscience* **29**, 2626–2636.

[47] Young ED, Robert JM, Shofner WP. 1988 Regularity and latency of units in ventral cochlear nucleus: Implications for unit classification and generation of response properties. *Journal of Neurophysiology* **60**, 1–29.

[48] Enroth-Cugell C, Shapley R. 1973 Adaptation and dynamics of cat retinal ganglion cells. *Journal of Physiology* **233**, 271–309.

[49] Drew PJ, Abbott LF. 2006 Models and properties of power-law adaptation in neural systems. *Journal of Neurophysiology* **96**, 826–833.

[50] Garson J. 2015 The Birth of Information in the Brain: Edgar Adrian and the Vacuum Tube. *Science in Context* **28**, 31–52.

[51] Consilience powers the big scientific ideas. https://www.abc.net.au/radionational/programs/scienceshow/consilience-powers-the-big-scientific-ideas/5111610. Accessed: 2021-03-17.

[52] Baylin F. 1979 Temporal patterns and selectivity in the unitary responses of olfactory receptors in the tiger salamander to odor stimulation. *Journal of General Physiology* **74**, 17–36.

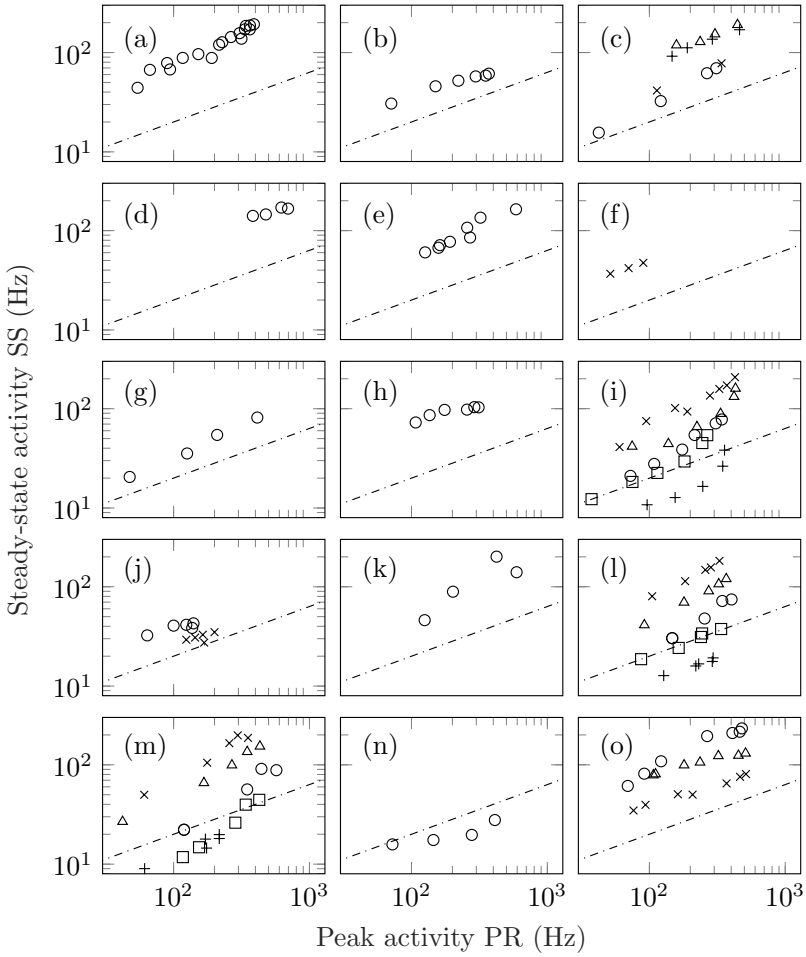

Figure 2: Steady-state activity (SS) plotted as a function of peak activity (PR) for different stimulus intensities. In all panels, the dashed line shows the predictions of equation (1) which is a line with slope one-half on a log-log plot. The value of the intercept depends on the precise value of the unit's spontaneous activity. (a) Plot of SS vs PR for auditory data taken from a single guinea pig fibre (figure 1, unit GP-17-4 [22]); (b) the same for auditory data from a single gerbil fibre (figure 1, unit E8F2 [23]); (c) results for four separate guinea pig auditory fibres of both high and low spontaneous activity (triangles, figure 1, unit GP31/08; plusses, figure 2, unit GP27/18; circles, figure 1, GP31/13; crosses, figure 2, GP27/04 [24]); (d) the averaged auditory data from ferrets (figure 6, [25]); (e) auditory responses obtained from the saccular nerve fibres of a gold fish (figure 3, increment [26]); (f) responses from lateral line in fish (figure 6, [21]) (g) stretch response in crayfish (figures 1 and 2, both PR and SS are shifted upwards by 0.5 log units [27]); (h) stretch response in frog (figure 3, both PR and SS are shifted upwards by 1 log unit [28]); (i) response of olfactory receptor neurons in fruit flies (figure 3a: crosses, shifted +0.3 log units; figure 5: triangles, shifted +0.1 log units, methyl butyrate; circles, shifted −0.1 log units, methyl butyrate; squares, shifted −0.3 log units, 1-pentanol; plusses, shifted −0.5 log units, propyl acetate [29]); (j) taste recordings in fruit fly sensilla (circles, figure 3; crosses, figure 7 [30]); (k) taste response in caterpillar (figure 3 [31]); (l) taste response in blowfly (figure 2a: circles, LiCl, shifted +0.2 log units; triangles, NaCl; crosses, KCl, shifted −0.2 log units; squares, RbCl, shifted −0.4 log units; plusses, CsCl, shifted −0.6 log units [32]); (m) same as (l) but for figure 2b [32]; (n) response to cooling in beetles (figure 10 [5]); and (o) vision data from a single ON-centre ganglion cell in the cat. The vision data differ from the other auditory data in that they are derived from pre-adapted luminance values (figure 7: circles, $1 \times 10^{-5}\,\mathrm{cd\,m^{-2}}$, shifted +0.2 log units; plusses, $1 \times 10^{-3}\,\mathrm{cd\,m^{-2}}$; crosses: $1 \times 10^{-1}\,\mathrm{cd\,m^{-2}}$, shifted −0 2 log units [33]).

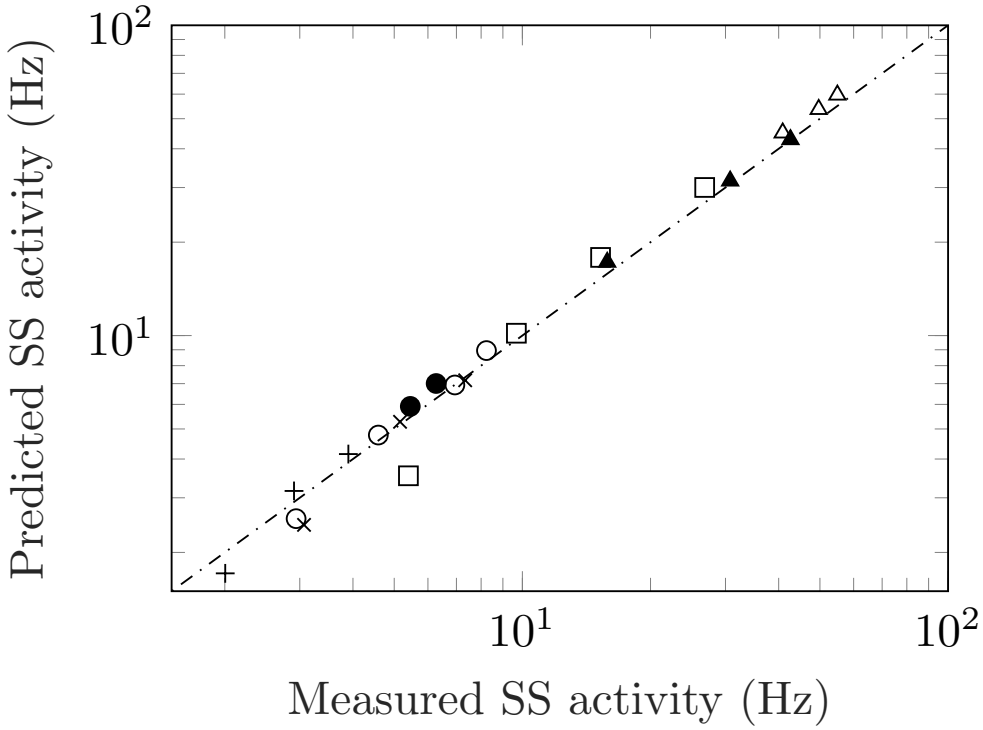

Figure 3: Measured versus predicted steady-state activity for ascending and descending staircases. Data from an ascending staircase of temperatures in warm units of cats (crosses, figure 2a [34]) and bats (squares, figure 2 [35]); response of M1 ipRGC in mice to an ascending/descending luminance staircase (open/filled circles, figures 1b/c [36]); ascending/descending staircases of acetone concentrations from olfactory sensory neurons in fruit flies which show both regular and inverted responses (open/filled triangles, figure 2c [37]). Finally, the inverted responses from cold fibres to a descending temperature staircase (plusses, figure 2 [38]).